RSC Advances

ROYAL SOCIETY OF CHEMISTRY

www.rsc.org/advances

Graphical abstract

Immobilization and Molecular Rearrangement of Ionic Liquids on the Surface of Carbon Nanotubes

Cuifang Zhao,[a,b] Baozeng Ren,[a] Yuting Song,[b] Junling Zhang,[b] Lingchao Wei,[a] Shimou Chen,[*b] Suojiang Zhang[*b]

Two kinds of imidazolium ionic liquids with different weight ratios were absorbed on the outer surface of MWCNTs. The orientational order and properties of ILs immobilized on the MWCNTs surface were analyzed.

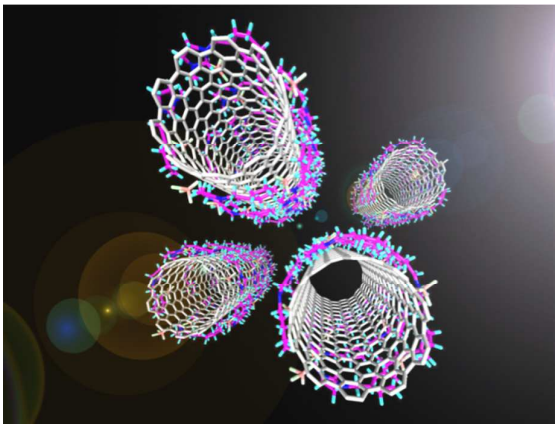

Journal Name RSCPublishing

ARTICLE

Immobilization and Molecular Rearrangement of Ionic Liquids on the Surface of Carbon Nanotubes

Cite this: DOI: 10.1039/x0xx00000x

Cuifang Zhao,[a,b] Baozeng Ren,[a] Yuting Song,[b] Junling Zhang,[b] Lingchao Wei,[a] Shimou Chen,[*b] Suojiang Zhang[*b]

Received 00th,
Accepted 00th

DOI: 10.1039/x0xx00000x

www.rsc.org/

Abstract

Two imidazolium-based ionic liquids (ILs), i.e. [Bnmim][BF_4] (1-benzyl-3-methylimidazolium tetrafluoroborate) and [Bmim][$AuCl_4$] (1-butyl-3-methylimidazolium chloroauric acid), were adsorbed on the outer surface of multi-walled carbon nanotubes (MWCNTs) via physical method. In order to understand the molecular packing of ILs immobilized on the MWCNTs surface, the composite samples with different weight ratios of ILs were characterized by using X-ray photoelectron spectroscopy (XPS), differential scanning calorimetry (DSC), X-ray diffraction (XRD) and Fourier transform infrared spectroscopy (FT-IR), respectively. It was found that the rings of imidazolium cations of ILs are nearly parallel to the MWCNTs surface, and the packing orientation is determined by the substitute groups on the imidazolium-ring. Both the anions ($[BF_4]^-$ and $[AuCl_4]^-$) occupy an adjacent area with imidazolium cation to form neutral surface layer. Furthermore, for the immobilized ILs, the melting point (Tm) of [Bmim][$AuCl_4$] rises slightly, while the Tm of [Bnmim][BF_4] gets depressed. The molecular rearrangement and the melting points change of the immobilized ILs result from the complex interfacial interactions between the ILs and the MWCNTs surface.

Introduction

Room-temperature ionic liquids (ILs) are a special class of liquids solely composed of cations and anions. [1, 2] In general, cations or both cations and anions are large, and the cations have a low degree of symmetry. [3] Interest in the relationship between the structure and property of ILs is rapidly expanding due to its importance on design and selection of ILs for task-specific applications. Recently, the microstructures and properties of ionic liquids at interfaces have gained increasing attentions due to their relevance in the application of ILs in catalytic processes, heat transfer, biosensors, electrodes, lubricants, solar cells, etc. [4-7] Although these technologies have been developed, fundamental aspects of the structure and properties of ILs under interfacial effects have been relatively less studied. This is partly due to the recent emergence of the field and, more importantly, the difficulty of accessing this regime in a well-defined model experiments.

Wang et al. [8] investigated the distribution mechanism of single-walled carbon nanotubes in imidazolium-based ILs by the combination of spectroscopic characterizations and molecular dynamics simulations, justifying that the dispersion was induced by weak van der Waals forces. By using surface-enhanced Raman spectroscopy (SERS), Rubim et al.[9] found that when [Bmim][BF_4] adsorbed on the Ag nanoparticles, the BMI^+ cation interacts chemically with the nanoparticle surface in a flat configuration, while the BF_4^- anions form a second negatively charged layer without interacting with Ag. Shim et al. [10] studied 1-ethyl-3-methyl imidazolium tetrafluoroborate solvation of single and multi-walled carbon nanotubes, showing a cylindrical distribution of the ions can form on the outer surface of nanotube, while the distribution of ions inside the nanotubes was dependent on the tube diameter. Santiago et al. [11] also reported that choline-based ILs cylindrical distributions around nanotubes and the adsorption layers were not uniform for the anions and cations. Steinrück, et al. investigated the ILs interfaces and related bulk properties by X-ray photoelectron spectroscopy (XPS), detailed information on surface orientation, enrichment effects, cation-anion interactions, and the correlation to bulk properties of ILs (such as density and surface tension of ILs) were derived. [12] However, for the ILs at solid interface, the following questions are still unclear: What

about the molecular arrangement, and whether it dependents on its structural feature of the ILs? What is the possible mechanism of the molecular rearrangement? How the interfacial effects change the properties and performance of the ILs? All these points are very important to understand ILs at interfaces and to guide the applications of the ILs.

In previous work, we reported the structure of ILs on the inner surface of single-walled carbon nanotubes by using high-resolution transmission electron microscopy (HRTEM). [13] Herein, the microstructures and the melting points variation of ILs immobilized on the outer surface of MWCNTs are presented, mainly by X-ray photoelectron spectroscopy (XPS), transmission electron microscopy (TEM), differential scanning calorimetry (DSC), and powder X-ray diffraction (XRD). With these characterization methods, the mechanism of the ILs molecular rearrangement induced by the interfacial effect was proposed for the first time.

Results and discussion

According to our literature survey on the studies of the ILs at interfaces, the ILs at gas-IL or vacuum-IL interfaces have been widely studied, while the experimental techniques are relatively lack for investigating the solid-IL interface. [14-17] The major cause of this difference is because of the great difficulty of accessing the solid-liquid interface and distinguishing the influence of the solid substrates. Pensado et al. [18] investigated the different ILs at the liquid–vacuum interface by simulation, and found that the alkyl side chains of the cations tend to protrude toward the vacuum, with the imidazolium rings placed in the liquid. Nakajima et al. [19] investigated the liquid-vacuum interface of different 1-alkyl-3-methylimidazolium-TFSI ILs using high-resolution Rutherford backscattering spectroscopy, which indicates that the imidazolium ring stays perpendicular to the surface. Wherein, simulations on the IL-carbon interface were observed the imidazolium ring laying parallel to the surface. Steven Baldelli [17] demonstrated that the imidazolium ring is nearly parallel to the solid surface with a single layer by their sum frequency generation (SFG) studies, and the larger the anion size, the more imidazolium ring was tilted along the solid surface. These inconsistent observations of molecular orientation of ILs are interesting enough to deserve more attention. Moreover, many reported works only focused on the specific orientation feature of the cations of ILs at interface. [13, 20] But the properties of ILs at solid interfaces are determined by both anions and cations actually. So when the structure and behavior of ILs on interfaces were discussed, how the two kinds of ions were ordered or oriented on the surface should be considered at the same time.

2.1 Immobilization of ILs on the MWCNTs surface

[Bnmim][BF_4] and [Bmim][$AuCl_4$] with different weight ratios were mingled with MWCNTs by physical method (see details in experimental part). We chose these two ILs, because they have totally different substitute group on their imidazolium rings, but their anion-structure and melting-point are similar. Fig 1 shows the typical SEM and TEM images of [Bnmim][BF_4]/MWCNTs samples. The adsorption of ILs on the surface of MWCNTs can be observed. Our extensive examination of TEM micrographs reveals that the thickness of ILs layer on the MWCNTs surface is about 1nm when the weight ratios of [Bnmim][BF_4] is 1.0wt%; the thickness of ILs layer is 2~4nm for the 2.5wt% [Bnmim][BF_4]/MWCNTs sample, and the adsorption layer thickness is 4~10nm when the weight ratios of [Bnmim][BF_4] is 5.0wt%. These results indicated that the ILs films adsorbed on the MWCNTs surface are ultrathin and are dependent on the weight ratios of the ILs. Due to the molecular size of the [Bnmim][BF_4] is about 0.9nm (from our theoretical calculation on the optimized geometry of [Bnmim][BF_4] at B3LYP/6-31+G(d,p) level). Thus, the single-molecular layer immobilization of [Bnmim][BF_4] can be obtained when the IL weight ratio is just or lower than 1.0wt%. As we know, the interfacial effects will play a key role at the adjacent layer between immobilized ILs and MWCNTs. When the thickness of the immobilized ILs is about 1nm, the sample can be regarded as an ideal sample for investigating the ILs at interfaces. With the loading weight ratio increasing, the ratio of the adjacent ILs at interfaces is decreased, and finally when we measure the ILs/MWCNTs samples by some experimental techniques (for example, XPS, FT-IR, XRD, etc), we can only obtain the signals of the bulk ionic liquid when the weight ratio is very high, due to in this case the contributions of the adjacent ILs layer in the signals almost can be ignored.

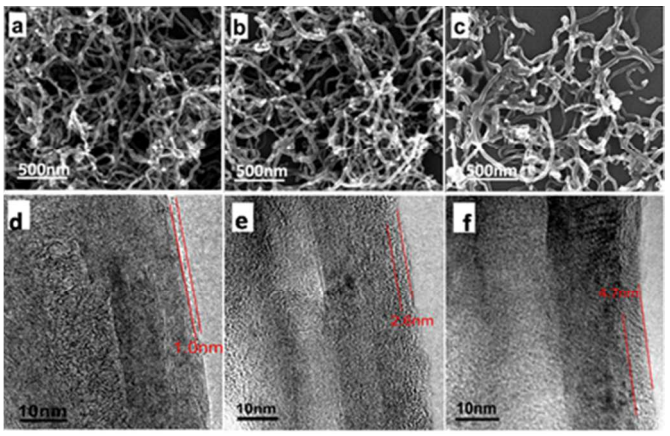

Fig 1. SEM and TEM images of different weight ratios of [Bnmim][BF_4] immobilized on the MWCNTs surface (ILs/MWCNTs). SEM: (a) 1.0wt% [Bnmim][BF_4]/MWCNTs, (b) 2.5wt% [Bnmim][BF_4]/MWCNTs, (c) 5.0wt% [Bnmim][BF_4]/MWCNTs. TEM: (d) 1.0wt% [Bnmim][BF_4]/MWCNTs, (e) 2.5wt% [Bnmim][BF_4]/MWCNTs, (f) 5.0wt% [Bnmim][BF_4]/MWCNTs. The calculated thicknesses of the immobilized [Bnmim][BF_4] in d, e and f are 1.0, 2.6, and 4.7nm, respectively.

2.2 Orientation features of the immobilized ILs

Fig 2A shows the XPS spectra of the C1s region for a series weight ratios of [Bnmim][BF_4] adsorption on the surface of MWCNTs. As we know, there are slightly different characteristic binding energies of the same kind elements in different chemical environments. Due to the different carbon

environments from the full C1s XPS cannot be distinguished; fitting procedures to decompose C1s spectra into different components should be developed. Herein, C_{alkyl} are aliphatic carbons or aromatic carbons and C_{hetero} are carbons bonded to at least one heteroatom in imidazolium ring. [21] Based on the XPS analysis on typical imidazolium-based ILs by Lovelock et al, [22] the peak of C_{alkyl} is at a lower bonding energy (BE) than that of the C_{hetero}. The peak at about 285.3eV can be attributed to the C_{alkyl}, and the peak at about 286.6eV can be assigned to C_{hetero}. [23-25] The graphitic C1s peak ($C_{graphite}$) is at about 284.2eV. As shown in Fig 2A, all the samples give a multicomponent C1s spectrum with two BE components for the bulk [Bnmim][BF_4] (C_{hetero} at 286.4eV; C_{alky} at 285.1eV) and three BE components for [Bnmim][BF_4]/MWCNTs sampleas (the third peak at 284.1eV are $C_{graphite}$ from MWCNTs). From our TEM analysis (Fig 1), the majority of adsorbed [Bnmim][BF_4] will form a monolayer coating on the surface of MWCNTs when the mass of the [Bnmim][BF_4] is 1.0wt%. In the case of monolayer adsorption, the orientation of the ILs will be strongly influenced by the interfacial interaction, and the signals of XPS only come from the adjacent ILs at the interface. Wherein, for the multi-layer adsorbed samples ([Bnmim][BF_4] is 5.0wt%), the adsorbed [Bnmim][BF_4] is much thicker than that of the monolayer, which means majority signals of the XPS come from the multilayer of the ILs, which not influenced by interfacial effects. In our experiments, when the mass ratio of the [Bnmim][BF_4] is 5.0wt%, the thickness of the adsorbed layer is about 4~10nm (Fig 1). In this case, the contribution of the adjacent ILs to the XPS almost can be ignored, that is why we found the ratios of the C_{alkyl}/C_{hetero} in the XPS spectra of the bulk [Bnmim][BF_4] and 5.0wt% [Bnmim][BF_4]/MWCNTs (which the area ratio of the C_{alkyl}/C_{hetero} is 1.37:1) were almost same (Fig 2A-a and 2A-b).Wherein, the ratios of the C_{alkyl}/C_{hetero} increase clearly when the weight ratio of the ILs is 2.5wt% (which the area ratio of the C_{alkyl}/C_{hetero} is 1.65:1, Fig 2A-c), which indicates that the interfacial effects become represented in this case. However, it is almost the same when the ratios further down to 1.0wt% (which the area ratio of the C_{alkyl}/C_{hetero} is 1.66:1, Fig 2A-d), which means the degree of the rearrangement of the[Bnmim][BF_4]/MWCNTs on the surface of MWCNTs in these two cases is similar. It means that at the outer surface of MWCNTs, the imidazolium ring is adsorbed along the surface, and the phenyl ring is a little titled along the MWCNTs.

In order to draw a full picture on the ion packing of [Bnmim][BF_4] on MWCNTs surface, we also investigated the signals of the anoin. Fig 2B shows the XPS spectra of the B and F region for the bulk [Bnmim][BF_4] and different weight ratios of [Bnmim][BF_4]/MWCNTs. The BE of B and F change with the mass ratios of [Bnmim][BF_4] on the MWCNTs surface which demonstrated the anions with different chemical environments at the interface. [25] That is to say the chemical state of the $[BF_4]^-$ changes in the surface region, which may influence by the interfacial effects. Furthermore, Fig 3 shows the intensity ratio for the core atom B from the anion, and the two nitrogen atoms from the imidazolium ring, the nominal ratio is 0.5 based on the chemical structure of [Bnmim][BF_4]. Both the bulk [Bnmim][BF_4] and [Bnmim][BF_4]/MWCNTs samples give the similar intensity ration of the two atoms, which indicate that the mean center of the anion in the surface region is located almost at the same distance from the outer MWCNTs surface, as compared with the imidazolium ring. [26] This data can also prove that anions and cations adsorb without decomposition. [27] Overall, the $[BF_4]^-$ anion should occupy an area with imidazolium cation to form a neutral surface layer. Similar phenomenon also reported by C. Kolbeck when they

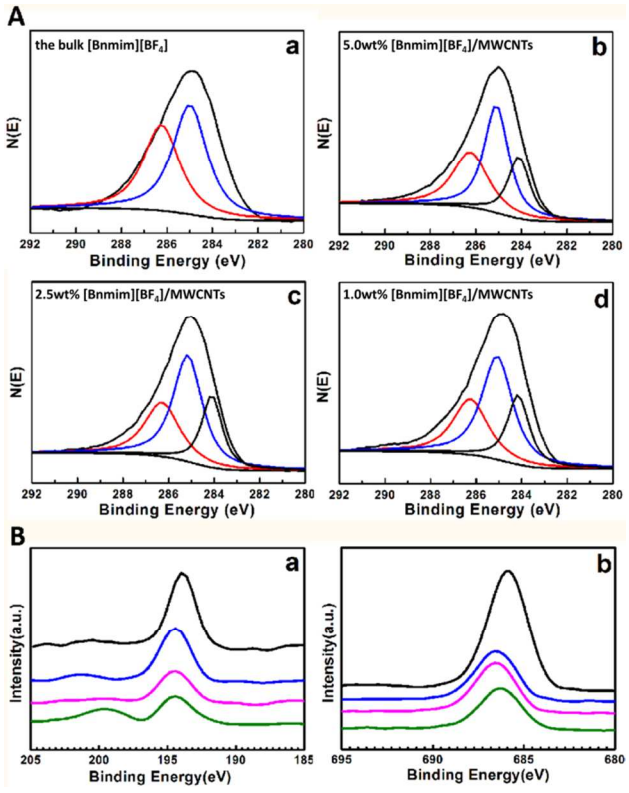

Fig 2. (A) The XPS of C1s region for different weight ratios of [Bnmim][BF_4] immobilized on the surface of MWCNTs. The red peak stands for C_{hetero} (C_{hetero} are carbons bonded to at least on N which contain in imidazolium ring), the black line is $C_{graphite}$ and the blue peak for C_{alkyl} (C_{alkyl} are carbons of aromatic ring). (B) B1s (a) and F1s (b) XPS of [Bnmim][BF_4]/MWCNTs. (Black) the bulk [Bnmim][BF_4], (Blue) 5.0wt% [Bnmim][BF_4]/MWCNTs, (Pink) 2.5wt% [Bnmim][BF_4]/MWCNTs, (Olive) 1.0wt% [Bnmim][BF_4]/MWCNTs.

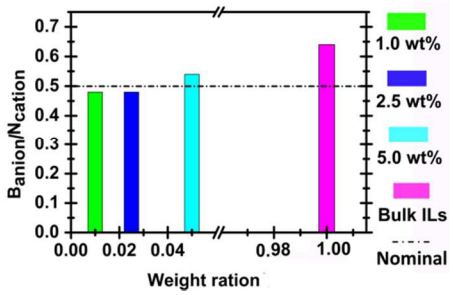

Fig 3. Ratios of the intensities B_{anion}/N_{cation} for 1.0wt% [Bnmim][BF_4]/MWCNTs, 5.0wt% [Bnmim][BF_4]/MWCNTs, 2.5wt% [Bnmim][BF_4]/MWCNTs and the bulk [Bnmim][BF_4].

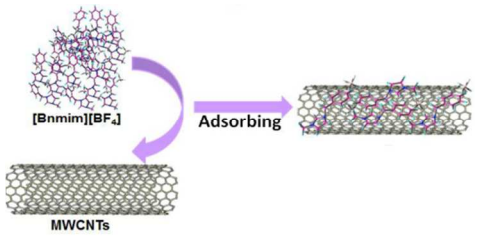

Fig 4. Scheme of [Bnmim][BF_4] on the outer surface of MWCNTs.

study the ILs at the Au surface. [26] A schematic diagram of the packing of the [Bnmim][BF_4] on the MWCNTs surface was shown in Fig 4.

To further investigate the influence of the cation-structure on the degree of rearrangement of the ILs on solid-liquid interface, another ILs with a carbon chain on the imdazolium ring, [Bmim][$AuCl_4$], was also immobilized on the surface of MWCNTs. From our TEM analysis, the thickness of the adsorbed [Bmim][$AuCl_4$] layers on MWCNTs surface also dependent on the weight ratio of the [Bmim][$AuCl_4$], which is similar to that of [Bnmim][BF_4] (TEM data not shown). The XPS spectra of the C1s region for a series weight ratios of [Bmim][$AuCl_4$] adsorption on the surface of MWCNTs are shown in Fig 5A. Similar with the cases of [Bnmim][BF_4] immobilized on the surface of MWCNTs, when the mass of the [Bmim][$AuCl_4$] is 1.0wt% (which the area ratio of the C_{alkyl}/C_{hetero} is 1.65:1), the majority of adsorbed [Bmim][$AuCl_4$] will form a monolayer, and when the mass of the [Bmim][$AuCl_4$] over 1.0wt% (in the cases of 2.5wt% and 5.0wt%), the adsorbed [Bmim][$AuCl_4$] will form multi-layer on MWCNTs surface. We found that the ratio of the C_{alkyl}/C_{hetero} increases with the decrease of the mass ratio of [Bmim][$AuCl_4$] on the MWCNTs surface (Figure 5A) (the area ratio of the C_{alkyl}/C_{hetero} is 0.84:1 when the mass of the [Bmim][$AuCl_4$] is 5.0wt%. and changed to 1.05:1 when the mass of the [Bmim][$AuCl_4$] is 2.5wt%.). It means that at the nanotube-ILs interface, the imidazolium ring tended to align parallel to the MWCNTs surface, while alkyl carbon chains prefer to perpendicular to the horizontal plane of the imidazolium ring and MWCNTs surface.

Furthermore, Fig 5B shows the XPS spectra of the Au and Cl region for the bulk [Bmim][$AuCl_4$] and different weight ratios of [Bmim][$AuCl_4$]. The BE of Au and Cl change slightly with the different mass ratios of [Bmim][$AuCl_4$], which indicates the $[AuCl_4]^-$ anions have different chemical states due to the interfacial effect. Fig 6 shows the intensity ratio for the core atom Au from the anion, and the two nitrogen atoms of the imidazolium ring, the nominal ratio is about 0.5 for the four samples, indicated that the anoin located almost at the same distance from the outer surface of MWCNTs when compared to the imidazolium ring (similar with the case of [Bnmim][BF_4]/MWCNTs, see for Fig 4). [26] It suggests that the imidazolium rings and anions are located almost at the same distance from the outer MWCNTs surface. [27] The schematic diagram of the packing of the [Bmim][$AuCl_4$] on the MWCNTs surface was shown in Fig 7.

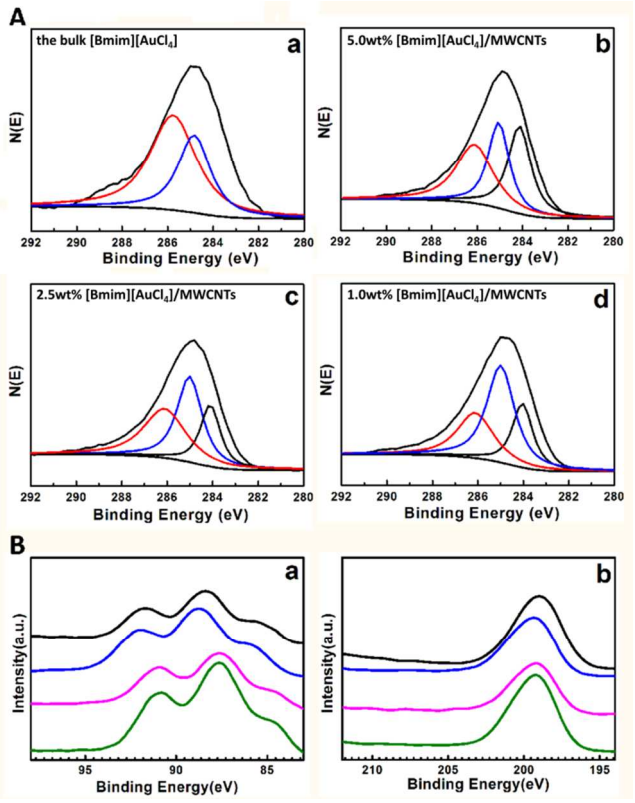

Fig 5. (A) C1s XPS spectra of a series weight ratios of [Bmim][$AuCl_4$] immobilized on the surface of MWCNTs. The red line stands for C_{hetero} (C_{hetero} are carbons bonded to at least one N in imidazolium ring), the black line is $C_{graphite}$ and the blue line is C_{alkyl} (C_{alkyl} are aliphatic carbons). (B) Au4f7 (a) and Cl2p3 (b) XPS spectra of the [Bmim][$AuCl_4$]/MWCNTs. (Black) the bulk [Bmim][$AuCl_4$], (Blue) 5.0wt% [Bmim][$AuCl_4$]/MWCNTs, (Pink) 2.5wt% [Bmim][$AuCl_4$]/MWCNTs, (Olive) 1.0wt% [Bmim][$AuCl_4$]/MWCNTs.

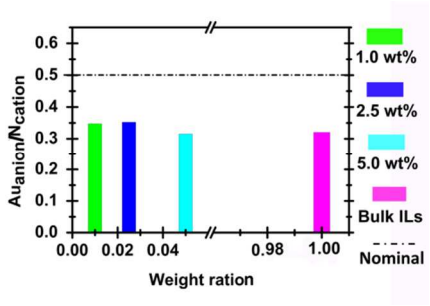

Fig 6. Ratios of the intensities Au_{anion}/N_{cation} for 1.0wt% [Bmim][$AuCl_4$]/MWCNTs, 5.0wt% [Bmim][$AuCl_4$]/MWCNTs, 2.5wt% [Bmim][$AuCl_4$]/MWCNTs and the bulk [Bmim][$AuCl_4$].

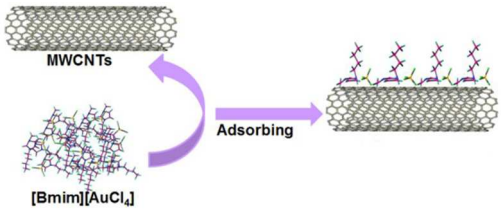

Fig 7. Scheme of [Bmim][$AuCl_4$] on the MWCNTs surface.

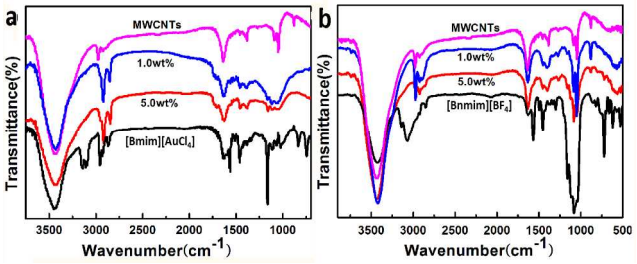

Fig 8. FT-IR spectra of bulk IL, MWCNTs and different weight ratios of ILs immobilized on the MWCNTs surface (a) [Bmim][$AuCl_4$], (b) [Bnmim][BF_4].

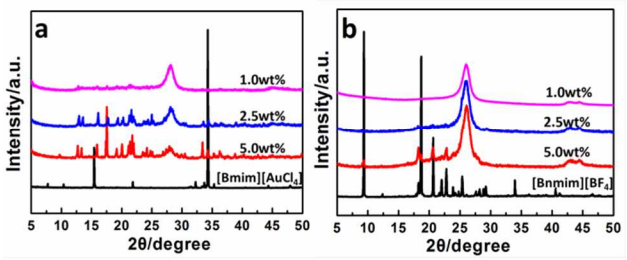

Fig 9. X-ray diffraction patterns for bulk IL and different weight ratios of ILs immobilized on the MWCNTs surface, (a) [Bmim][$AuCl_4$], (b) [Bnmim][BF_4], (Black) the bulk IL, (Red) 5.0wt% ILs, (Blue) 2.5wt% ILs, (Magenta) 1.0wt% ILs.

Although the models of the ILs/MWCNTs interface (see in Fig 4 and 7) have been put forward, it is unknown why the immobilized ions ordered in that way. It has been reported that some imdazolium-based ILs molecule can adsorb on carbon nanotube sidewalls through weak intermolecular H-bonding, π-π stacking, van der Waals, electrostatic, and other interactions. [28] Wang et al. [29] studied the mechanism of SWCNTs dispersed in imidazolium-based ILs, and found that the ILs interact with SWCNTs through weak van der Waals interaction and π-π stacking. Herein, the imidazolium and aromatic ring can be induced by the π-electrons on the MWCNTs surface, it is speculated that the molecular orientation of ILs on the MWCNTs surface is triggered by the complex interactions between the ILs and MWCNTs. The interactions were confirmed by FT-IR. As shown in Fig 8, IR spectra of a series weight ratios of [Bmim][$AuCl_4$] and [Bnmim][BF_4] immobilized on the surface of MWCNTs were compared with those of the bulk ILs. For the bulk ionic liquid, the imidazolium ring is surrounded by several anions that are connected with the interactions between ions. [30] Different with the bulk [Bmim][$AuCl_4$] and MWCNTs, when [Bmim][$AuCl_4$] is immobilized onto the MWCNTs surface, the peak of stretching vibration disappeared from 3100~3200cm^{-1} (Fig 8a). And the peak of imidazalium ring (2986, 3074cm^{-1}) is shifting. So for the ILs, the interaction between cations and ations changed after the ILs immobilized on the MWCNTs. The red shifted of some peak, suggesting a changed surrounding between [Bmim][$AuCl_4$] and the MWCNTs surface. These denote there are interactions between MWCNTs surface and ILs, and which induce the arrangement of the ILs immobilized on the surface of MWCNTs. For [Bnmim][BF_4]/MWCNTs samples (Fig 8b), similar with the above case, the interactions should exist between [Bnmim][BF_4] and MWCNTs. On the other hand, for the FTIR spectra of MWCNTs (after disposing of H_2SO_4 and HNO_3) in Fig. 8, the absorption band at 3420cm^{-1} is assigned to the stretching vibration of H_2O, the peak at 2980cm^{-1} according to the exciting of -COOH group, 1640cm^{-1} attributed to the C=O vibration, and 1050cm^{-1} is ascribed to the stretching vibration of C-O. For the FTIR spectra of [Bmim][$AuCl_4$]/MWCNTs, the peaks of the stretching vibration of H_2O, the C=O vibration and the stretching vibration of C-O is at 3440, 1630 and 1110cm^{-1}, respectively. Comparing with that of MWCNTs, the shifts of these three peaks are 20, 10 and 50cm^{-1}, respectively. Indicating the complex interaction between [Bmim][$AuCl_4$] and MWCNTs may be existed.[29] The results of FT-IR characterizations further confirm the rearrangement of the ILs on the MWCNTs surface due to the interfacial effects.

2.3 The structure related to crystallization behavior

To elucidate the role and influence of the interfacial effect on the crystallization behavior of the ILs on the MWCNTs surface, the X-ray diffraction (XRD) technique was employed. Many researchers have studied the diffraction pattern of the purified MWCNTs, showing that the sharp peak position at 26.4° and other weak peak at about 42.0° which correspond to the (002), (100) planes of graphitized MWCNTs, respectively. [31] Herein, XRD patterns for the different weigh ratios of [Bmim][$AuCl_4$]/MWCNTs and [Bnmim][BF_4]/MWCNTs are shown in Fig 9. Compared with the bulk [Bmim][$AuCl_4$], many new diffraction peaks appear in XRD patterns (Fig 9a), and the relative intensity of the X-ray diffraction peak changes clearly at some points. It indicates that a polymorphous solid phase of [Bmim][$AuCl_4$] is formed on the surface of MWCNTs. As the weight ratios of the immobilized [Bmim][$AuCl_4$] and [Bnmim][BF_4] are low, especially in the case of lower than 2.5wt% loading amount, the ILs/MWCNTs interface might affect the molecular orientation of the ILs. For the [Bnmim][BF_4]/MWCNTs, both imidazolium and aromatic could parallel to the surface of MWCNTs to form a cation-π interaction. [32] The results are in good agreement with our XPS analysis. As mentioned above, some interactions of the MWCNTs surface with ILs could influence the orientation of [Bmim][$AuCl_4$] and [Bnmim][BF_4]. In addition, this speculation also is consistent with the conclusion by previous studies. [33, 34] The weak interactions at interfaces was suggested to inducing the structure of immobilized ILs on the surface ordered, and resulted in the aberrational diffraction of XRD patterns.

2.4 Phase behavior of the immobilized ionic liquids

The phase behavior of the two different ILs immobilized on the MWCNTs was investigated by DSC. As shown in Fig 10a, there is a slight difference of the first melting point (at about 54.9°C) between the immobilized [Bmim][$AuCl_4$] and the bulk [Bmim][$AuCl_4$]. For the 5.0wt% [Bmim][$AuCl_4$]/MWCNTs,

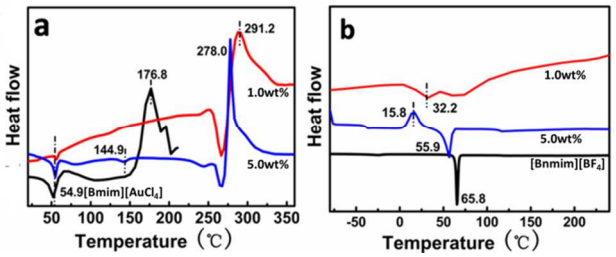

Fig 10. DSC traces of [Bmim][$AuCl_4$]/MWCNTs and [Bnmim][BF_4]/MWCNTs in compared with the bulk IL, (a) [Bmim][$AuCl_4$], (b) [Bnmim][BF_4].

the second melting point appears at 144.9°C, indicating that the new phase formed when [Bmim][$AuCl_4$] adsorbed on the MWCNTs surface. The observation is similar to that of the 1.0wt% [Bmim][$AuCl_4$]/MWCNTs. Furthermore, at high temperature region, the DSC thermograms of 5.0wt% [Bmim][$AuCl_4$]/MWCNTs and 1.0wt% [Bmim][$AuCl_4$]/MWCNTs show a pyrolysis peak at 278.0°C and 291.2°C, respectively, which are much higher than those of [Bmim][$AuCl_4$] in bulk (decomposition temperature ~176.8°C). These results further confirm the complex interfacial interactions existing between the ILs and the MWCNTs surface[35, 36] with the new phase formation. On the contrary, as shown in Fig 10b, the immobilization of [Bnmim][BF_4] on the MWCNTs surface leads to a decrease in the melting point. The 5.0wt%[Bnmim][BF_4]/MWCNTs shows an endothermic peak at 55.9°C, which downshifts about 15.8°C as compared with the bulk [Bnmim][BF_4] (Tm~66.2°C), and further decreased to 32.2°C for 1.0wt% [Bnmim][BF_4]/MWCNTs. According to the mean field theory used for analysis the melting point changing for the ionic liquids in our previous work, [36, 37] the observation suggests that the molecular packing and the interfacial effects are different for these two kinds of immobilized ILs. The [Bmim][$AuCl_4$] may closely packed on the surface of MWCNTs, wherein, the [Bnmim][BF_4] may loosely adsorbed on the surface of MWCNTs due to the bulky benzyl groups on the imidazolium ring.

Experimental

3.1 Materials

[Bmim][$AuCl_4$] and [Bnmim][BF_4] ILs were purchased from Shanghai Chengjie Chemical Co., with 99.0% purity. The ILs were purified carefully in our laboratory by recrystallization and the purity was confirmed by ^{1}H NMR and HPLC. The properties of ILs are known to change with purity, particularly the water content. Therefore, the ILs were preheated at 70°C in vacuum for 48h before using. The multi-walled carbon nanotubes (MWCNTs) were obtained from Chengdu Organic Chemical Co. (99.0% purity, with mean diameter of 10~20nm).

3.2 Sample preparation

The MWCNTs were purified as follows: A certain amount of H_2SO_4 and HNO_3 with volume ratio of 3:1 were mixed with moderate MWCNTs in a glass beaker. The mixture was put in the ultrasonic cleaner (400W, with a setting temperature of 70°C) for 6h. Then the MWCNTs were received by washing, suction filtration and drying. After getting rid of amorphous carbon by calcination at high temperature (1100°C) in tube furnace under argon flow for 4h, the high purity MWCNTs were obtained without defects and functional groups on the outer surface.

In order to study the microstructures and properties of the immobilized ILs on the surface of MWCNTs, [Bmim][$AuCl_4$] and [Bnmim][BF_4] were selected as two typical ILs, one with alkyl substituent group, the other with benzyl conjugated group on the imidazolium-ring. For getting the different thickness layer of immobilized ionic liquid on the MWCNTs surface, different weight ratios (1.0, 2.5, and 5.0wt% of ILs) of ILs/MWCNTs samples were prepared by dissolving certain amount of MWCNTs and ILs in methanol (20ml), followed by removing the methanol via putting the mixture in the ultrasonic cleaner, after about 10 h, most of the solvent volatilized and the ILs uniformly adsorbed on the MWCNTs surface. All the obtained samples were dried in vacuum at 60°C for 48 h to remove volatiles completely. For simplicity, the final samples were named [Bmim][$AuCl_4$]/MWCNTs and [Bnmim][BF_4]/MWCNTs for the two kinds immobilized ILs, respectively.

3.3 Characterizations

Scanning electron microscope (SEM) measurements were carried out with a XL30 S-FEG. Transmission electron microscopy (TEM) was performed using a JEOL JEM 2100F microscope. The samples for TEM observations were prepared by putting the solid powder on the micro grid copper net, followed by blowing the copper grids by nitrogen.

The XPS spectra were obtained by using an XPS spectrometer (ESCA-300; Scienta, Uppsala, Sweden) with a monochromatized Al Kα X-ray source ($h\nu$ =1486.6eV) at a power of 2.4kW and a base pressure of 7.3×10^{-8}Pa in the analytical chamber. The analyzer slit width and the pass energy was 0.5mm and 150eV, respectively. All the samples were prepared by placing little sample on the aluminum foil with permanent double sided tape, and then pressing them into films as thin as possible. After thin film preparation, the samples were carried into preparation chamber and pumped to high vacuum pressure for avoiding significant absorption of volatile impurities. After 3-4h, the samples transferred to the main analytical vacuum chamber to collect data. For data interpretation, the samples were analyzed with XPSPEAK41 by fitting C1s spectra after Shirley background subtraction. The XPS spectra were charge corrected by referencing the containment carbon (C1s = 284.8eV). To aid visual analysis of the XPS spectra presented in the text, the spectra are normalized to the fitted area of C1s, and the peaks are due to the carbon atom in the cations of ILs and MWCNTs. These peaks were selected to be used for normalization, and the carbon contribution from either the cations of ILs or MWCNTs studied here distinguish by binding energy. [38] This normalization is applied to all XPS spectra for the samples. The peak at 285.3eV is fitted with one component, C_{alkyl}, the peak at 286.6eV is C_{hetero}, and the peak at 284.2eV is $C_{graphite}$.

Phase behaviors of the bulk and immobilized ILs were measured by DSC (DSC1, Mettler-Toledo Corp.). Samples (about 4~8mg) were placed in aluminium pans with pierced lids at a heating rate of 10°C/min in N_2 atmosphere.

The FT-IR spectra of samples were measured on a Nicolet infrared spectrophotometer 380.

Conclusions

Two kinds of imidazolium ionic liquids with different weight ratios were adsorbed on the outer surface of MWCNTs. The orientational order and properties of ILs immobilized on the MWCNTs surface were analysed by XPS, XRD, DSC, and FT-IR, respectively. For the [Bmim][$AuCl_4$]/MWCNTs, the ring of [Bmim][$AuCl_4$] cation is in parallel with the MWCNTs surface, and the alkyl chains prefer to orient out into the bulk, and there was an enrichment of the cations at the adjacent interface. However, for the [Bnmim][BF_4]/MWCNTs, both the imdazolium ring and the phenyl substitute group on the ring tend to lay flat on the MWCNTs surface. For the anions, $[AuCl_4]^-$ and $[BF_4]^-$ are located almost at the same distance from the outer MWCNTs surface as compared to the imdazolium ring. In addition, the phase transition behavior of the two different ILs immobilized on the MWCNTs was investigated by DSC. The melting point of [Bmim][$AuCl_4$] rises slightly, while the melting piont of the immobilized [Bnmim][BF_4] gets depressed. The rearrangement and the melting points change of the immobilized ILs are due to the complex interfacial interactions and the packing density of the two ILs. We believe that these results are important for instruction of many IL applications in which solid-liquid interface are involved.

Acknowledgements

This work was supported by National Natural Science Foundation of China (No. 21276257, 21210006, 51104140) and Beijing Natural Science Foundation (2132054).

Notes

[a] School of Chemical Engineering and Energy, Zhengzhou University, Zhengzhou 450001, Henan, P. R. China.

[b] Beijing Key Laboratory of Ionic Liquids Clean Process, Key Laboratory of Green Process and Engineering, State Key Laboratory of Multiphase Complex Systems, Institute of Process Engineering, Chinese Academy of Sciences, Beijing 100190, P. R. China. E-mail: chenshimou@home.ipe.ac.cn; sjzhang@home.ipe.ac.cn

References

1 T. Welton, *Coord. Chem. Rev.*, 2004, **248**, 2459-2477.
2 K. Binnemans, *Chem. Rev.*, 2005, **105**, 4148-4204.
3 M. J. Earle and K. R. Seddon, *Pure Appl. Chem.*, 2000, **72**, 1391-1398.
4 T. Katakabe, T. Kaneko, M. Watanabe, T. Fukushima and T. Aida, *J. Electrochem. Soc.*, 2005, **152**, A1913-A1916.
5 C. A. Nieto de Castro, M. J. V. Lourenço, A. P. C. Ribeiro, E. Langa and S. I. C. Vieira, *J. Chem. Eng. Data*, 2010, **55**, 653-661.
6 R. T. Kachoosangi, M. M. Musameh, I. Abu-Yousef, J. M. Yousef, S. M. Kanan, X. Lei, S. G. Davies, A. Russell and R. G. Compton, *Anal. Chem.*, 2009, **81**, 435-442.
7 L. Ding, T. He, Y. Xiong, J. Wu, L. Chen and G. Chen, *Prog. Chem.*, 2010, **22**, 298-308.
8 J. Wang, H. Chu and Y. Li, *ACS Nano*, 2008, **2**, 2540-2547.
9 J. C. Rubim, F. A. Trindade, M. A. Gelesky, R. F. Aroca and J. Dupont, *J. Phys. Chem. C*, 2008, **112**, 19670-19675.
10 Y. Shim and H. J. Kim, *ACS Nano*, 2009, **3**, 1693-1702.
11 S. Aparicio, M. Atilhan, *J. Phys. Chem. C*, 2012, **116**, 12055-12065.
12 H.-P. Steinrück, *Phys. Chem. Chem. Phys.*, 2012, **14**, 5010-5029.
13 S. Chen, K. Kobayashi, Y. Miyata, N. Imazu, T. Saito, R. Kitaura and H. Shinohara, *J. Am. Chem. Soc.*, 2009, **131**, 14850-14856.
14 H.-P. Steinrück, J. Libuda, P. Wasserscheid, T. Cremer, C. Kolbeck, M. Laurin, F. Maier, M. Sobota, P. S. Schulz and M. Stark, *Adv. Mater*., 2011, **23**, 2571-2587.
15 M. J. Skaug, J. Mabry and D. K. Schwartz, *Phys. Rev. Lett.*, 2013, **110**, 256101.
16 F. Zaera, *Surf. Sci.*, 2011, **605**, 1141-1145.
17 S. Baldelli, *J. Phys. Chem. Lett*., 2013, **4**, 244-252.
18 A.S. Pensado, M. F. Costa Gomes, J. N. Canongia Lopes, P. Malfreyt and A. A. H. Padua, *Phys. Chem. Chem. Phys.*, 2011, **13**, 13518-13526
19 K. Nakajima, A. Ohno, H. Hashimoto, M. Suzuki and K. Kimura, *J. Chem. Phys.*, 2010, **133**, 044702 (1-7).
20 C. Y. Penalber, Z. Grenoble, G. A. Baker and S. Baldelli, *Phys. Chem. Chem. Phys.*, 2012, **14**, 5122-5131.
21 K. R. J. Lovelock, I. J. Villar-Garcia, F. Maier, H.-P. Steinrueck and P. Licence, *Chem. Rev.*, 2010, **110**, 5158-5190.
22 K. R. J. Lovelock, C. Kolbeck, T. Cremer, N. Paape, P. S. Schulz, P. Wasserscheid, F. Maier and H.-P. Steinrück, *J. Phys. Chem. B*, 2009, **113**, 2854-2864.
23 N. Kocharova, T. Aaritalo, J. Leiro, J. Kankare and J. Lukkari, *Langmuir*, 2007, **23**, 3363-3371.
24 S. Frey, A. Shaporenko, M. Zharnikov, P. Harder and D. L. Allara, *J. Phys. Chem. B*, 2003, **107**, 7716-7725.
25 F. Maier, T. Cremer, C. Kolbeck, K. R. J. Lovelock, N. Paape, P. S. Schulz, P. Wasserscheid and H.-P. Steinrück, *Phys.Chem.Chem.Phys.*, 2010, **12**, 1905-1915.
26 C. Kolbeck, C. Tremer, K. R. J. Lovelock, N. Paape, P. S. Schulz, P. Wasserscheid, F. Maier and H.-P. Steinrück, *J. Phys. Chem. B*, 2009, **113**, 8682-8688.
27 F. Buchner, F. T. Katrin, U. Benedikt, A. Dorothea, W. Nadja, F. Hanieh, G. Axel and R. J. Behm, *ACS Nano*, 2013, **7**, 7773-7784.
28 N. Kocharova, J. Leiro, J. Lukkari, M. Heinonen, T. Skala, F. Sutara, M. Skoda and M. Vondracek, *Langmuir*, 2008, **24**, 3235-3243.
29 J. Wang, H. Chu and Y. Li, *ACS Nano*, 2008, **2**, 2540-2546.
30 J. DuPont, P. A. Z. Suarez, R. F. De Souza, R. A. Burrow and J. P. Kintzinger, *Chem.Eur.J.*, 2000, **6**, 2377-2381.
31 Y. Zhang, S. Qi and F. Zhang, *Mater. Res. Bull.*, 2012, **47**, 3743-3746.
32 T. Fukushima. A. Kosaka, Y. Ishimura, T. Yamamoto, T. Takigawa, N. Ishii and T. Aida, *Science*, 2003, **300**, 2072-2074.
33 P. Vishweshwar, A. Nangia and V. M. Lynch, *Growth Des.*, 2003, **3**, 783-790.
34 W. Huang and H. Qian, *J. Mol. Struct.*, 2007, **832**, 108-116.
35 L. Rodriguez-Perez, Y. Coppel, I. Favier, E. Teuma, P. Serp and M. Gomez, *Dalton Trans.*, 2010, **39**, 7565-7568.
36 S. Chen, G. Wu, M. Sha and S. Huang, *J. Am. Chem. Soc.*, 2007, **129**, 2416-2417.
37 S. Chen, Y. Liu, H. Fu, Y. He, C. Li, W. Huang, Z. Jiang and G. Wu, *J. Phys. Chem. Lett.*, 2012, **3**, 1052-1055.
38 S. Men, B. B. Hurisso, K. R. J. Lovelock and P. Licence, *Phys. Chem. Chem. Phys.*, 2012, **14**, 5229-5238.

TOC: